Redox Biology 28 (2020) 101364

Contents lists available at ScienceDirect

Redox Biology

journal homepage: www.elsevier.com/locate/redox

# The nuclear transcription factor FoxG1 affects the sensitivity of mimetic aging hair cells to inflammation by regulating autophagy pathways

Zu-hong He[a,1], Sheng-yu Zou[a,1], Ming Li[a], Fu-ling Liao[a,f], Xia Wu[a], Hai-ying Sun[a], Xue-yan Zhao[a], Yu-juan Hu[a], Dan Li[a], Xiao-xiang Xu[g], Sen Chen[a], Yu Sun[a,*], Ren-jie Chai[b,c,d,e,h,**], Wei-jia Kong[a,***]

[a] Department of Otorhinolaryngology, Union Hospital, Tongji Medical College, Huazhong University of Science and Technology, Wuhan, 430022, China
[b] Key Laboratory for Developmental Genes and Human Disease, Ministry of Education, Institute of Life Sciences, Southeast University, Nanjing, 210096, China
[c] Co-Innovation Center of Neuroregeneration, Nantong University, Nantong, 226001, China
[d] Institute for Stem Cell and Regeneration, Chinese Academy of Science, Beijing, China
[e] Jiangsu Province High-Tech Key Laboratory for Bio-Medical Research, Southeast University, Nanjing, 211189, China
[f] Xiangyang Central Hospital, Affiliated Hospital of Hubei University of Arts and Science, Xiangyang, 441021, China
[g] Otorhinolaryngology, Head and Neck Surgery, Zhongnan Hospital of Wuhan University, Wuhan, 430071, China
[h] Beijing Key Laboratory of Neural Regeneration and Repair, Capital Medical University, Beijing, 100069, China

A B S T R A C T

Inflammation is a self-defense response to protect individuals from infection and tissue damage, but excessive or persistent inflammation can have adverse effects on cell survival. Many individuals become especially susceptible to chronic-inflammation-induced sensorineural hearing loss as they age, but the intrinsic molecular mechanism behind aging individuals' increased risk of hearing loss remains unclear. FoxG1 (forkhead box transcription factor G1) is a key transcription factor that plays important roles in hair cell survival through the regulation of mitochondrial function, but how the function of FoxG1 changes during aging and under inflammatory conditions is unknown. In this study, we first found that FoxG1 expression and autophagy both increased gradually in the low concentration lipopolysaccharide (LPS)-induced inflammation model, while after high concentration of LPS treatment both FoxG1 expression and autophagy levels decreased as the concentration of LPS increased. We then used siRNA to downregulate *Foxg1* expression in hair cell-like OC-1 cells and found that cell death and apoptosis were significantly increased after LPS injury. Furthermore, we used D-galactose (D-gal) to create an aging model with hair cell-like OC-1 cells and cochlear explant cultures *in vitro* and found that the expression of *Foxg1* and the level of autophagy were both decreased after D-gal and LPS co-treatment. Lastly, we knocked down the expression of *Foxg1* under aged inflammation conditions and found increased numbers of dead and apoptotic cells. Together these results suggest that FoxG1 affects the sensitivity of mimetic aging hair cells to inflammation by regulating autophagy pathways.

## 1. Introduction

Inflammation is a beneficial host defense response to protect individuals from infection and tissue damage. When the host discovers that pathogens and tissue damage are present, it initiates an inflammatory response in an attempt to at least partially return the organism to its normal phenotype [1]. In contrast to the beneficial effects of acute inflammation, chronic low-grade inflammation is a crucial contributor to various age-related pathologies and natural processes in aging tissues and plays a role in the development of cardiovascular disease [2], type II diabetes [3], and Alzheimer disease [4].

A particularly under-researched field is the effect of such chronic inflammation on presbycusis, or age-related hearing loss [5,6]. It is known that the permeability and structure of the round window membrane changes with long-term infection [7], and this can allow lipopolysaccharide (LPS) to pass through the round window membrane and into the inner ear [8]. LPS is a key molecule in the outer membrane of gram-negative bacteria that triggers an inflammatory response in the host organism. When LPS enters the inner ear it can induce inflammatory cell recruitment [9], stria vascularis swelling, and hair cell

* Corresponding author. Department of Otorhinolaryngology, Union Hospital of Tongji Medical College, Huazhong University of Science and Technology, Wuhan, 430022, China.
** Corresponding author. Co-Innovation Center of Neuroregeneration, Key Laboratory for Developmental Genes and Human Disease, Ministry of Education, Institute of Life Sciences, Southeast University, Nanjing, 210096, China.
*** Corresponding author. Department of Otorhinolaryngology, Union Hospital of Tongji Medical College, Huazhong University of Science and Technology, Wuhan, 430022, China.
*E-mail addresses:* sunyu@hust.edu.cn (Y. Sun), renjiec@seu.edu.cn (R.-j. Chai), entwjkong@hust.edu.cn (W.-j. Kong).
[1] These authors contributed equally to this work.

https://doi.org/10.1016/j.redox.2019.101364
Received 17 August 2019; Received in revised form 22 October 2019; Accepted 27 October 2019
Available online 29 October 2019

(HC) damage [10] thus leading to sensorineural hearing loss [11]. The migration of mononuclear phagocytes to the inner ear in response to such insults might play an important role in hearing and balance dysfunction, and with the release of inflammatory mediators such cells might affect inner ear function in the short or long term [12,13]. Mononuclear phagocytic cells enter the spiral ligament when the mice are treated with LPS, resulting in an increase in the number of CCR2(+) inflammatory monocytes in the inner ear, which in turn causes the cochlear inflammatory response [14,15]. Therefore, when LPS-induced inflammation becomes severe or persistent, the cochlear blood-labyrinth barrier will be disrupted and cause pathological changes in the inner ear, including bleeding and inflammatory cell recruitment, eventually lead to hearing loss [16–18].

Oxidative stress is an important part of the inflammatory response, and mitochondria are the main site of cellular ROS production. The production of ROS occurs mainly in the mitochondrial oxidative respiratory chain, thus mitochondrial structural and functional disorders can lead to mitochondrial ROS accumulation [19]. These active oxygen radicals cause damage to macromolecules such as proteins and DNA, which in turn trigger the degradation of tissues and organs [20]. In the inner ear, oxidative stress and mitochondrial abnormalities caused by excessive ROS production play an important role in the development of senile deafness [21,22], and previous studies have shown that mitochondrial mtDNA common deletion (CD) mutations are directly related to degenerative changes in the auditory system and can lead to increased sensitivity of the auditory system to ototoxic drugs and noise [23,24]. However, the molecular mechanism through which aging HCs exhibit greater sensitivity to external inflammatory stress remains unclear.

As integral parts of the normally functioning immune system, mitochondrial ROS function synergistically with nuclear transcription factors (such as NF-κB, Sirt1, Nrf2, and HMGB1) to regulate the progression of inflammation [25–27]. The forkhead family member FoxG1 is an important transcription factor that regulates cell proliferation and differentiation, and mutations in the *Foxg1* gene affect axon and neuron development and differentiation [28]. During inner ear development, FoxG1 is important for maintaining the formation of inner ear sensory HCs [29] and for ensuring normal cochlear morphology [30], and in our previous study we found that knockout of *Foxg1* in HCs negatively affects cell survival during the postnatal period. FoxG1 is also known to regulate mitochondrial energy metabolism and biosynthesis [31–33], and thus abnormal expression of FoxG1 will have negative consequences for mitochondrial function. As the main site of energy metabolism in eukaryotic cells, mitochondria have a wide range of biological functions, including the regulation of cell proliferation, differentiation, apoptosis, and aging. We hypothesize, therefore, that FoxG1 plays an important role in processes related to aging and inflammation.

An important process in regulating inflammation and in responding to the cellular damage induced by ROS is autophagy, which is a highly conserved process in all eukaryotic cells. This cellular recycling process provides raw materials to the cell through the ordered degradation of senescent and dysfunctional organelles and is critical for maintaining cell homeostasis [34]. Mitochondrial autophagy, also known as mitophagy, is important for the removal of damaged mitochondria and for the maintenance of cellular mitochondrial network function, and it has an anti-inflammatory effect. However, the regulation mechanism of autophagy under inflammatory conditions has not been completely clarified, although it is known that inflammation activates autophagy to eliminate pathogens [35,36]. Thus autophagy can protect cells against inflammatory injury by inhibiting the activation of the inflammasome and by suppressing pro-inflammatory signaling pathways [37,38]. However, recent research has shown that the level of autophagy decreases with aging [39], and this might play a role in age-related hearing loss.

In this study, in order to reveal the effects and mechanisms of FoxG1 in protecting against inflamm-aging–related HC degeneration, we took advantage of the D-gal–induced mimetic aging HC-like OC1 cell line and aging mouse cochlear explant cultures to investigate the role of FoxG1 in HC survival *in vitro*. We found that FoxG1 expression as well as autophagy level were first gradually increased with low-concentration LPS treatment, but sharply decreased with high-concentration LPS treatment. Furthermore, we explored the relationship between FoxG1 and the autophagy pathways and showed that FoxG1 regulated the autophagy pathways and maintained intracellular homeostasis and resisted external stress in mimetic aging HCs.

## 2. Results

### 2.1. The survival of HC-like OC1 cells decreased as LPS concentration and treatment time increased

To construct the LPS-induced HC-like OC-1 cell inflammation model, we determined the optimum LPS treatment to induce HC damage. We first treated the OC-1 cells with different LPS concentrations (1 μg/mL, 5 μg/mL, 10 μg/mL, 20 μg/mL, 30 μg/mL, 40 μg/mL, 50 μg/mL, 60 μg/mL, 70 μg/mL, 80 μg/mL, and 100 μg/mL) for 48 h. The CCK8 results showed that the cell density was significantly decreased compared to the controls when the concentration of LPS was higher than 5 μg/mL (Supplement Figure 1A, $p < 0.05$, n = 3). We used propidium iodide to label the dead cells and Annexin V to label the cells undergoing apoptosis and found that the proportions of both dead and apoptotic cells were significantly increased compared to controls as the concentration of LPS increased (Supplement Fig. 1B–D, $p < 0.001$, n = 3). To determine the appropriate treatment time of LPS, we used 1 μg/mL LPS to treat OC-1 cells for different times (24 h, 48 h, 72 h, and 96 h). The flow cytometry results showed that the proportions of both dead and apoptotic cells were significantly increased compared to the undamaged controls when the 1 μg/mL LPS treatment time was 48 h or longer (Supplement Fig. 1 E–G, $p < 0.05$, n = 3). TUNEL staining showed significantly greater proportions of apoptotic cells compared to controls when the 1 μg/mL LPS treatment time was 48 h or longer (Supplement Fig. 1H–I, $p < 0.001$, n = 3). Moreover, we determined whether the inflammatory response was activated in OC-1 cells after LPS treatment. We measured the production of three well-known proinflammatory cytokines – TNFα, IL-1β, and IL-6 – by ELISA in OC-1 cells and cell culture supernatant after 1 μg/mL LPS treatment for 48 h. Compared with controls, TNFα and IL-1β showed non-significant increases in LPS-induced production of IL-1β and TNFα in the supernatant; however, IL-6 was significantly increased in the supernatant after LPS treatment (Supplement Fig. 1J, $p < 0.05$, n = 3). These results suggested that 1 μg/mL LPS treatment for 48 h led to an appropriate level of damage and inflammation activation in OC-1 cells, so we used this LPS concentration and time for all of the experiments in this study.

### 2.2. Oxidative stress increased in OC-1 cells as LPS treatment time increased

Because mitochondria are both an important source of ROS and a target for ROS damage, mitochondria play an important role in the development and progression of inflammation [40,41]. We used MitoSOX Red to detect mitochondrial ROS levels in OC-1 cells after 1 μg/mL LPS treatment for different times (24 h, 48 h, 72 h, 96 h). Flow cytometry and immunohistochemistry both showed that the ROS levels were increased compared to controls with increasing LPS treatment time (Supplement Fig. 2A–C, $p < 0.001$, n = 3).

### 2.3. Construction of the D-gal–induced HC-like OC-1 aging model

The OC-1 cells were analyzed for various aging phenotypic changes after 15 mg/mL D-galactose (D-gal) treatment for 72 h. TEM imaging

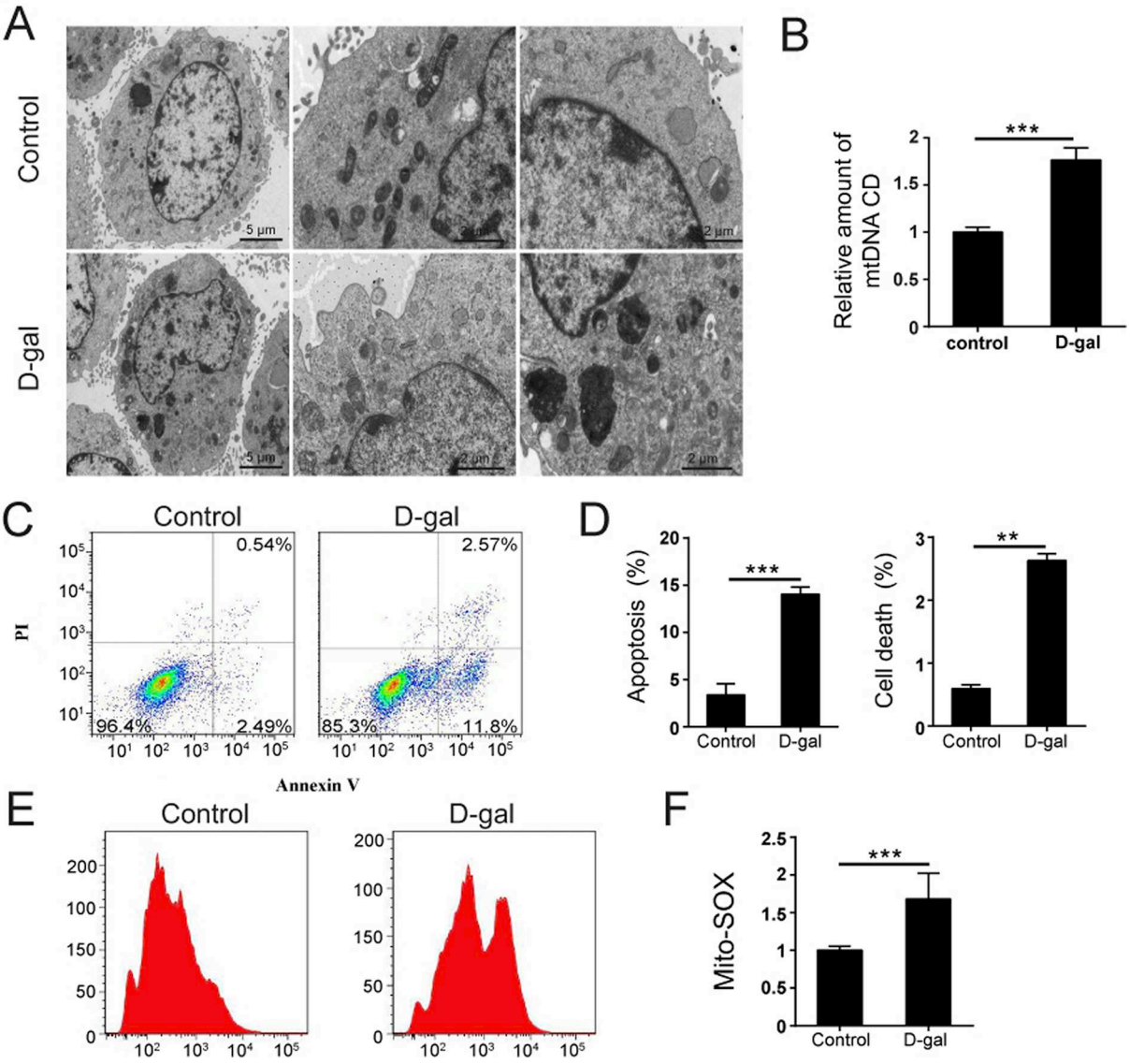


**Fig. 1.** Phenotypic changes in OC-1 cells after treatment with 15 mg/mL D-gal for 72 h. (A) TEM analysis to evaluate aging in OC1 cells. (B) Measurement of the mitochondrial DNA (mtDNA) common deletion (CD) after D-gal treatment. (C) Apoptosis analysis by flow cytometry after D-gal treatments. (D) The proportions of early apoptotic cells and dead cells in C. (E) The results of ROS analysis by flow cytometry after D-gal treatments. (F) Quantification of the data in E. For all experiments, *p < 0.05, **p < 0.01, ***p < 0.001.

showed degeneration of the mimetic aging OC-1 cells, including a decrease in nucleus to nucleolus ratio, the formation of wrinkles in the nuclear membrane, and heterochromic chromatin condensation; the deposition of lipofuscin in the cytoplasm; and reduced mitochondrial number, abnormal mitochondrial morphology, and mitochondrial swelling (Fig. 1A). The mtDNA CD test in D-gal–induced aging cells showed that mtDNA loss was significant compared to controls (Fig. 1B, $p < 0.001$, n = 3), and after D-gal treatment the proportions of both dead and apoptotic cells were significantly increased compared to controls (Fig. 1C and D, $p < 0.001$, n = 3). Mito-SOX Red was used to detect mitochondrial ROS in D-gal–induced aging OC1 cells, and subsequent flow cytometry showed that the ROS levels were significantly increased compared to controls after D-gal treatment (Fig. 1E and F, $p < 0.001$, n = 3).

### 2.4. The susceptibility to LPS-induced inflammatory response increased in mimetically aging HCs

In order to study the LPS-induced inflammatory response in aging HCs, we dissected the cochleae from postnatal day (P)3 GFP-LC3B mice and cultured them with 10 mg/mL D-gal for 24 h and then co-treated them with 0.5 μg/mL or 2 μg/mL LPS for 48 h. Immunofluorescence staining for Myosin7a and DAPI showed that Myo7a-positive HC loss was increased in the cochlea after treatment with LPS and that co-treatment with D-gal significantly increased the LPS-induced HC loss (Fig. 2A and B, $p < 0.05$, n = 3).

### 2.5. The susceptibility to LPS-induced inflammatory response increased in D-gal-induced mimetic aging HC-like OC-1 cells

Previous studies have shown that D-gal–induced mtDNA CD mutations are directly related to degenerative changes in the auditory system and can lead to increased sensitivity of the auditory system to noise [33,34]. Thus we explored the changes in aging OC-1 cells' sensitivity to LPS-induced inflammatory responses. OC-1 cells were pretreated with 15 mg/mL D-gal for 24 h and then co-treated with 1 μg/mL LPS for 48 h. The flow cytometry results showed that the proportions of both dead and apoptotic cells were significantly increased in the D-gal group and

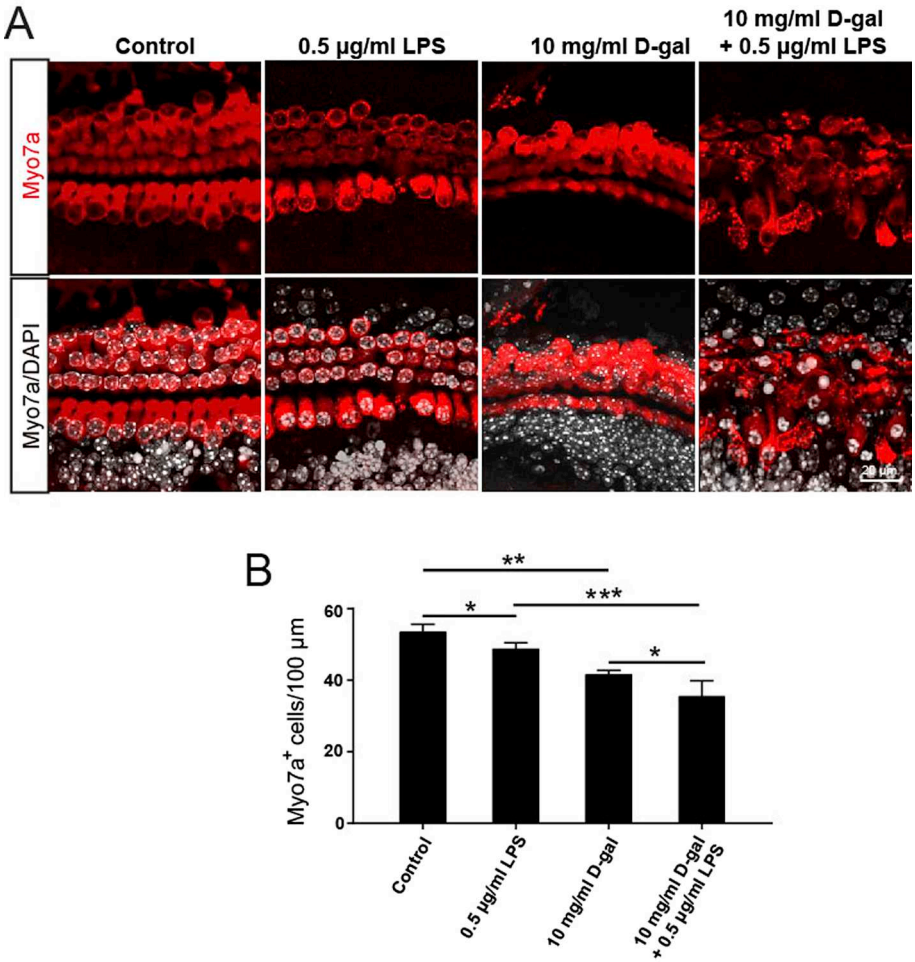


**Fig. 2.** The susceptibility to LPS-induced inflammatory response in D-gal–induced mimetic aging HCs was increased. (A) Immunofluorescence staining with Myo7a antibody in the D-gal–induced aging cochleae from GFP-LC3B mice after LPS treatment. (B) Quantification of the Myo7a-positive HCs in A, n = 3. For all experiments, *p < 0.05, **p < 0.01, ***p < 0.001.

the LPS group compared to controls (Fig. 3A–C, $p < 0.05$, n = 3). In the D-gal + LPS group, the proportion of apoptotic and dead cells was significantly increased compared to the D-gal–only group and the LPS-only group. TUNEL staining was consistent with the flow cytometry results, and the proportion of TUNEL-positive cells in the D-gal + LPS group was significantly increased compared to the D-gal–only group and the LPS-only group (Fig. 3D and E, $p < 0.01$, n = 3).

Mitochondrial structural and functional disorders can lead to mitochondrial ROS accumulation, which is an indicator of aging and apoptosis [42]. To test whether oxidative stress affects the sensitivity of aging cells to LPS-induced inflammatory response, we used Mito-SOX Red to evaluate mitochondrial ROS levels in OC-1 cells after different treatments. Flow cytometry and immunohistochemistry showed that the ROS levels were increased after D-gal or LPS treatment compared to the undamaged controls and that the ROS levels were increased even more in the D-gal + LPS group (Fig. 3F–H, $p < 0.01$, n = 3).

The mtDNA CD test showed that mtDNA loss was significantly increased compared to controls after D-gal treatment and that mtDNA loss was more severe after D-gal + LPS co-treatment, suggesting that mitochondrial damage is increased in aging cells under inflammatory conditions (Fig. 3I, $p < 0.001$, n = 3).

We also performed qPCR to analyze the mRNA expression of apoptosis-related genes, and we found that the expression of three pro-apoptotic marker genes (*FADD*, *Bax*, and *Aif*) was increased and that the expression of the anti-apoptotic gene *Bcl2* (B-cell lymphoma 2) was decreased in OC-1 cells after D-gal or LPS treatment compared to control cells, and this decrease was even greater in the D-gal + LPS group (Fig. 3J, $p < 0.05$, n = 3). The ratio of *Bcl2* to *Bax* also showed a decrease in the ratio in OC-1 cells after LPS or D-gal treatment. When the cells were treated with D-gal and LPS simultaneously, the ratio was decreased more significantly (Fig. 3K, $p < 0.05$, n = 3).

### 2.6. The expression of FoxG1 changed in OC-1 cells as the LPS treatment time increased

To determine if the expression of *Foxg1* is associated with inflammation, we treated the OC-1 cells with 1 μg/mL LPS for different treatment times (24 h, 48 h, 72 h, 96 h). The western blot results showed that the expression of *Foxg1* was increased when the cells were treated with LPS for 48 h but was significantly decreased when the cells were treated with LPS for 72 h or 96 h (Supplement Fig. 3A and B, $p < 0.05$, n = 3). Immunofluorescence staining with anti-FoxG1 showed that the expression of FoxG1 was increased when the cells were treated with LPS for 48 h compared with the control group and was significantly decreased when the cells were treated with LPS for 72 h or 96 h (Supplement Figure 3C). These results were consistent with the apoptosis data in Fig. 1, which showed that the apoptosis and cell death levels of OC-1 cells were not significantly increased when the LPS treatment time was less than 48 h, but were dramatically increased when the treatment time exceeded 48 h. These results suggest that FoxG1 plays an important protective role in the survival of OC-1 cells in the face of LPS-induced inflammatory injury, but when the cell damage

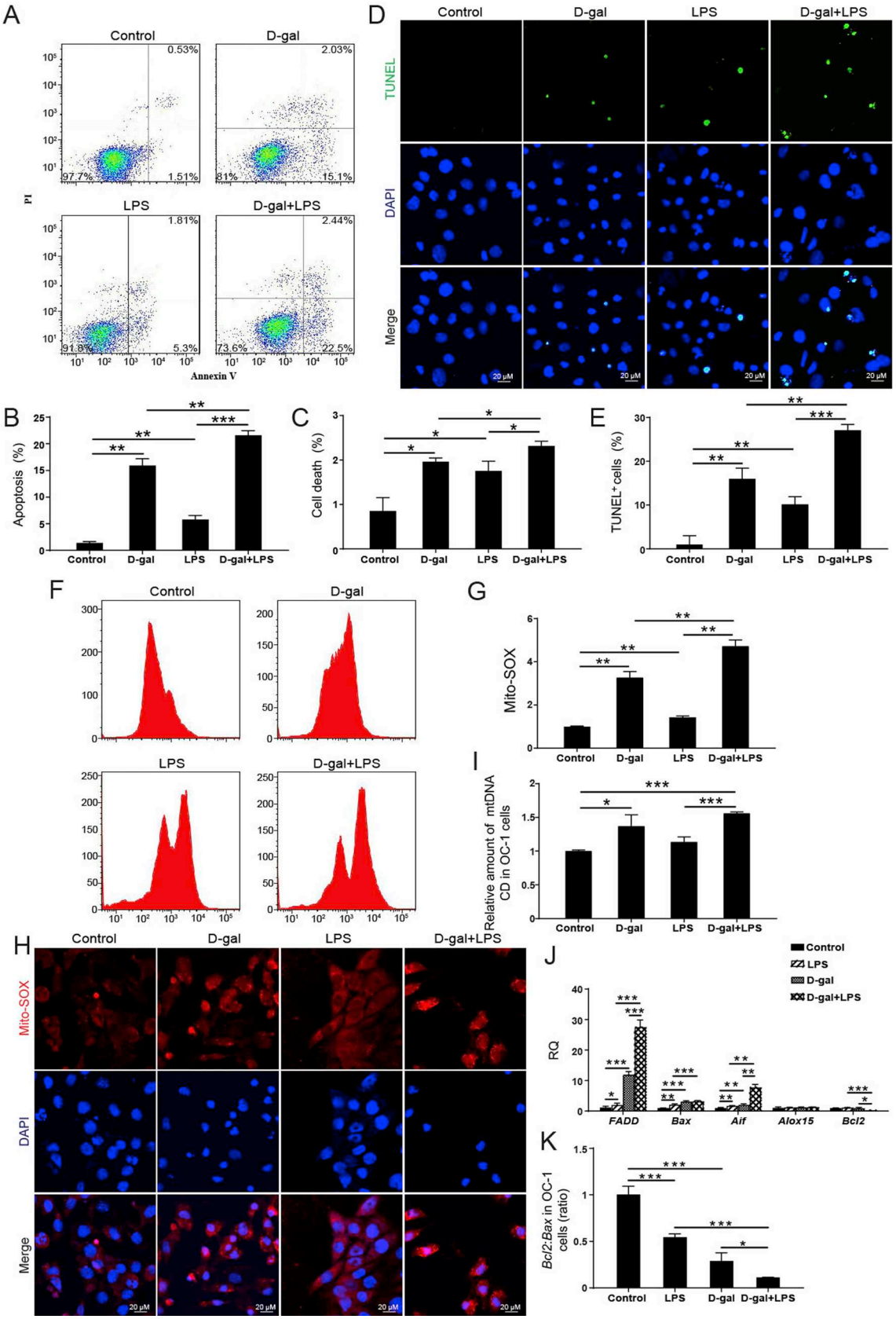


**Fig. 3.** The susceptibility to LPS-induced inflammatory response was increased in D-gal–induced mimetic aging cells. (A) Apoptosis analysis by flow cytometry after different treatments, n = 3. (B) The proportions of early apoptotic cells in A. (C) The proportions of dead cells in A. (D) TUNEL and DAPI double staining showing the apoptotic OC-1 cells after different treatments, n = 3. (E) Quantification of the numbers of TUNEL/DAPI double-positive cells in D. (F) Analysis of ROS levels by flow cytometry after different treatments. (G) Quantification of the data in F. (H) Immunofluorescence staining with Mito-SOX in OC-1 cells. (I) Measurement of mtDNA CD after different treatments. (J) qPCR analysis of apoptosis-related gene expression in OC-1 cells, n = 3. (K) The ratio of *Bcl2* to *Bax* in OC-1 cells after different treatments, n = 3. For qPCR experiments, the values for the untreated controls were set to 1. *p < 0.05, **p < 0.01, ***p < 0.001.

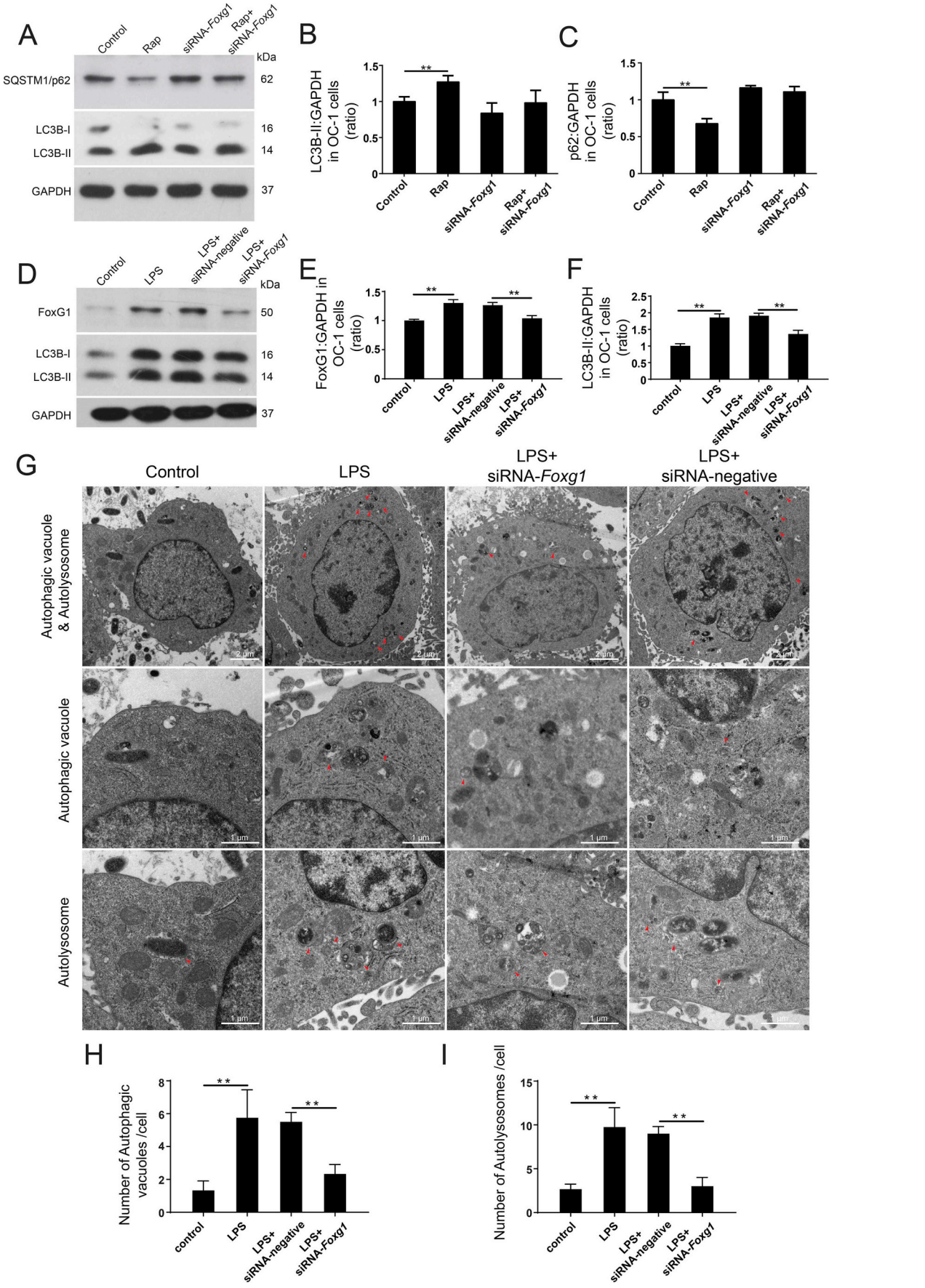


*(caption on next page)*

**Fig. 4.** The expression of FoxG1 affects autophagosome formation in OC-1 cells following 1 μg/mL LPS treatment for 48 h. (A) Western blot showing the changes in SQSTM1/p62 and LC3B expression in the OC-1 cells after Rap treatment, n = 3. (B) Quantification of the LC3B levels in A. (C) Quantification of the SQSTM1/p62 levels in A. (D) Western blot showing the changes in LC3B expression in OC-1 cells after downregulation of *Foxg1* expression following 1 μg/mL LPS treatment. (E) and (F) Quantification of the western blot in D. (G) Transmission electron microscope analysis for evaluating autophagy in OC-1 cells. (H) Quantification of the autophagic vacuoles in G. (I) Quantification of the autolysosomes in G. For all experiments, *p < 0.05, **p < 0.01, ***p < 0.001.

exceeds the cell's ability to repair it *Foxg1* expression is significantly reduced and apoptosis is significantly increased.

### 2.7. The level of autophagy changed in OC-1 cells as the LPS treatment time increased

When cells are exposed to external stress, the accumulation of mitochondrial damage leads to decreased mitochondrial membrane potential and increased ROS production [40]. Autophagy plays an essential role in cell survival by recycling damaged organelles and eliminating harmful substances [43], and because toxic substances and ROS are important factors in autophagy activation [34,44] we measured the expression of the autophagosome marker LC3B in OC-1 cells after 1 μg/mL LPS for different treatment times (24 h, 48 h, 72 h, 96 h). Western blots showed that the expression of LC3B was increased when cells were treated with 1 μg/mL LPS for less than 48 h, and the expression reached its peak when the cells were treated with LPS for 48 h, which suggested that LPS might trigger cytoprotective responses and activate autophagic signaling when the treatment time is less than 48 h (Supplement Fig. 4A and B, $p < 0.01$, n = 3). When the LPS treatment time was longer than 48 h, autophagy returned to similar levels as controls, indicating that cell self-protection was lost with extended LPS treatment time. These results were consistent with the significantly increased number of apoptotic cells and significantly decreased FoxG1 expression when the LPS treatment time was longer than 48 h. Therefore, we speculate that there is a synergistic regulatory relationship between FoxG1 and the autophagy pathway in the LPS-induced inflammatory response.

We also transfected OC-1 cells with the mRFP-GFP-LC3 plasmid, which is a reporter of autophagic flux, in order to detect changes in the numbers of autophagosomes and autolysosomes [45,46]. The numbers of both autophagosomes and autolysosomes were significantly increased compared to controls as the LPS treatment time increased to 48 h (Supplement Fig. 4C–E, $p < 0.001$, n = 3), and the numbers of autophagosomes and autolysosomes decreased as LPS treatment was extended past 48 h.

### 2.8. FoxG1 regulated the level of autophagy in OC-1 cells in response to LPS-induced inflammation

To further explore the relationship between FoxG1 and autophagy in OC-1 cells in response to LPS-induced inflammation, we determined the expression of LC3B and the degradation of the autophagic substrate SQSTM1/p62 protein when cells were treated with the autophagy activator rapamycin (Rap) and the expression of *Foxg1* was downregulated via siRNA transfection. The western blot data showed that the expression of LC3B was significantly increased and SQSTM1/p62 was significantly decreased after treatment with Rap compared with controls (Fig. 4A–C, $p < 0.01$, n = 3). We also found that after knockdown of *Foxg1*, the Rap-induced changes in LC3B and SQSTM1/p62 expression were not statistically significant, indicating that FoxG1 plays an important role in regulating autophagy processes and might be required for the activation of autophagy in OC-1 cells (Fig. 4A–C, $p < 0.01$, n = 3). In addition, we found that the expression of LC3B and FoxG1 was increased after treatment with 1 μg/mL LPS for 48 h compared with controls (Fig. 4D–F, $p < 0.05$, n = 3). In contrast, when the cells were treated with siRNA-*Foxg1* to inhibit FoxG1 expression the expression of LC3B was significantly reduced compared with LPS treatment alone.

To double confirm that FoxG1 regulates the autophagy pathway as part of the LPS-induced inflammatory response, we used TEM imaging to determine the changes in autophagy after downregulation of *Foxg1*. The LPS-treated cells had significantly more autophagic vacuoles (double membrane-bound autophagosomes) and autolysosomes (containing lysosomal membrane proteins and enzymes) compared with controls (Fig. 4G–I, $p < 0.01$, n = 3), and downregulation of FoxG1 resulted in significant inhibition of autophagy, indicating that autophagic flux in OC-1 cells is activated by FoxG1 after LPS treatment.

In addition, we also explored the effects of LPS-induced inflammation on the level of autophagy in cochlear HCs in adult mice. P40 GFP-LC3B mice were divided into two groups, the LPS-treated group and the normal saline group, with five in each group. Consistent with previous literature reports [47,48], P40 mice in the LPS-treated group were *trans*-tympanically injected with a 10 μl suspension of LPS in 0.9% sterile sodium chloride (LPS 2 mg/ml), and then allowed to recover for 72 h before analysis. Saline was injected in the control group. Immunofluorescence staining showed that the intensity of GFP-LC3 in HCs was significantly increased after LPS treatment compared to the controls (Fig. 5A and B, $p < 0.01$, n = 5). To further measure the protein expression level, the same experimental settings were used, and we dissected out the cochlea and performed a total protein extraction. The western blot showed that the expression of FoxG1 and LC3B were both significantly increased when the mice were treated with LPS, which was consistent with the results in HC-like OC-1 cells, indicating that LPS activates the pro-survival effects of FoxG1 and autophagy activity (Fig. 5C–E, $p < 0.05$, n = 3).

### 2.9. FoxG1 affected cell apoptosis and oxidative stress in OC-1 cells in response to LPS-induced inflammation

We have shown that FoxG1 can regulate autophagy activity, which has been reported to be an effective way to eliminate ROS and damaged mitochondria [34]. Therefore, we hypothesized that FoxG1 might affect cell apoptosis and oxidative stress in OC-1 cells in response to LPS-induced inflammation. First, we used Mito-SOX Red to evaluate the mitochondrial ROS levels in LPS-treated cells after downregulation of *Foxg1* expression. Flow cytometry and immunohistochemistry results showed that after downregulation of *Foxg1* the ROS levels were significantly increased compared to the control groups transfected with siRNA-negative (Fig. 6A–B, $p < 0.01$, n = 3). With the siRNA-*Foxg1* pretreatment, the ROS levels were reduced in OC-1 cells when autophagy was activated by Rap compared to the LPS + siRNA-*Foxg1* group, but the levels were still higher than the LPS + Rap group (Fig. 6A–B, $p < 0.05$, n = 3).

In order to determine the role of FoxG1 in OC-1 cell survival after LPS treatment, we pre-treated the cells with siRNA-*Foxg1* before LPS treatment. The flow cytometry results showed that after downregulation of *Foxg1* the proportions of both dead and apoptotic cells were significantly increased compared to the groups transfected with siRNA-negative (Fig. 6C–E, $p < 0.001$, n = 3). With the siRNA-*Foxg1* and Rap co-treatment, the proportions of both dead and apoptotic cells were significantly reduced in OC-1 cells compared to the LPS + siRNA-*Foxg1* group, but the proportions of apoptotic cells were still significantly increased compared to the LPS + Rap group (Fig. 6C–E, $p < 0.01$, n = 3).

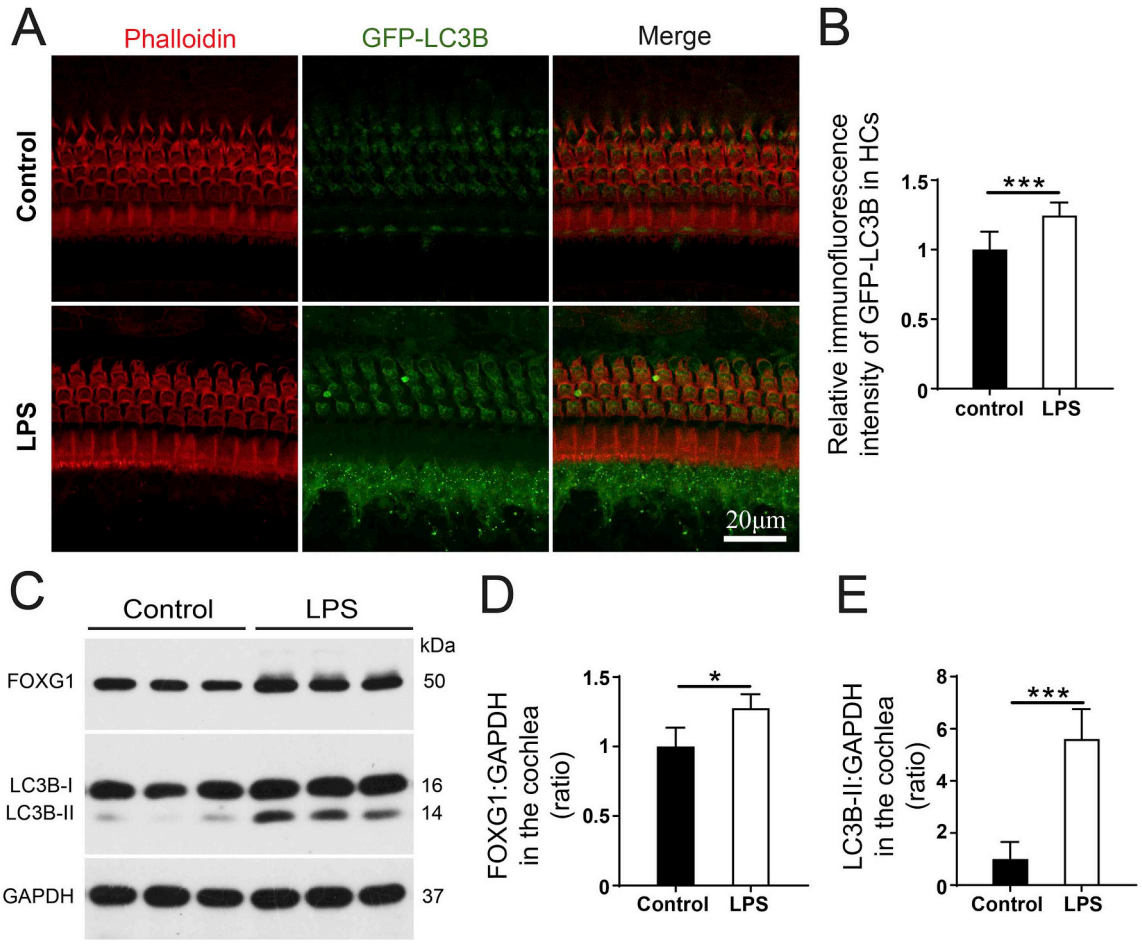


**Fig. 5.** FoxG1 expression and autophagy were activated in HCs after *trans*-tympanic injection of LPS. (A) Immunofluorescence staining with phalloidin in the cochlear HCs from GFP-LC3B mice after LPS treatment, n = 5. (B) Quantification of relative GFP-LC3B fluorescence intensity in HCs, normalized to control levels. (C) Western blot showing the changes in FoxG1 and LC3B expression in the HCs after different concentration of LPS treatment, n = 3. (D) and (E) Quantification of the western blot in C. For all experiments, *p < 0.05, ***p < 0.001.

### *2.10. FoxG1 regulated cochlear HC survival and reduced the susceptibility to LPS-induced inflammation by activating the autophagy pathway*

In order to confirm that FoxG1 protects HCs by activating autophagy, we dissected the cochleae from P3 GFP-LC3B mice and cultured them with different concentrations of LPS (0.1 μg/mL, 0.5 μg/mL, 1 μg/mL, and 2 μg/mL) for 48 h or with different concentrations of D-gal (1 mg/mL, 5 mg/mL, 10 mg/mL, 15 mg/mL, and 20 mg/mL) for 72 h. The western blot showed that the expression of FoxG1 and LC3B gradually increased when the LPS concentration was lower than 0.5 μg/mL, indicating that low concentrations of LPS might activate the pro-survival effect of FoxG1 as a self-protection mechanism (Fig. 7A–C, $p < 0.05$, n = 3). When the LPS concentration was higher than 1 μg/mL, the expression of FoxG1 and LC3B returned to similar levels as controls. In addition, we found that the expression of FoxG1 and LC3B decreased as the D-gal concentrations increased past 10 mg/mL, indicating that aging HCs lost their self-protection ability as the concentration of D-gal increased (Fig. 7D–F, $p < 0.05$, n = 3).

To further determine whether FoxG1 reduced the susceptibility to LPS-induced inflammation in aging HCs by activating the autophagy pathway, the cochleae of GFP-LC3 mice were cultured with 10 mg/mL D-gal for 24 h and then co-treated with 0.5 μg/mL or 2 μg/mL LPS for 48 h. The western blot showed that the expression of FoxG1 and LC3 was significantly decreased in the D-gal + LPS group compared to the LPS-only and D-gal–only groups, which was consistent with the *in vivo* data in Fig. 8. Immunofluorescence staining showed that the numbers of LC3 spots in each HC were significantly increased after 0.5 μg/mL LPS treatment compared to the controls (Fig. 7J and K, $p < 0.01$, n = 3). The results also showed that treatment with 10 mg/mL D-gal resulted in a reduction in the number of LC3 spots in HCs compared to controls, and co-treatment with D-gal and LPS markedly decreased the number of LC3 spots in HCs compared to the D-gal–only and LPS-only groups (Fig. 7J and K, $p < 0.01$, n = 3).

### *2.11. FoxG1 regulated the susceptibility of aging OC-1 cells to LPS-induced inflammation by activating autophagy*

Previous research reported that FoxG1 plays crucial roles in cell proliferation, differentiation, metabolism, apoptosis, and development by regulating ATP synthesis and metabolism in the mitochondria [33,49]. In our previous studies we found that FoxG1 promotes HC survival in the postnatal cochlea through the regulation of multiple signaling pathways [30]. Thus we hypothesized here that FoxG1 might reduce oxidative stress and apoptosis in D-gal–induced mimetic aging OC-1 cells after LPS treatment by activating the autophagy pathway. Because FoxG1 plays an important role in transcriptional regulation and mitochondrial function maintenance, in order to explore whether FoxG1 plays a role in HC aging we separated the nuclei and cytoplasm of OC-1 cells and measured the expression level of FoxG1 after D-gal treatment. The expression of FoxG1 was significantly decreased in the nuclei of D-gal–induced aging OC-1 cells (Supplement Fig. 5A–B, $p < 0.01$, n = 3). The expression level of FoxG1 also showed a

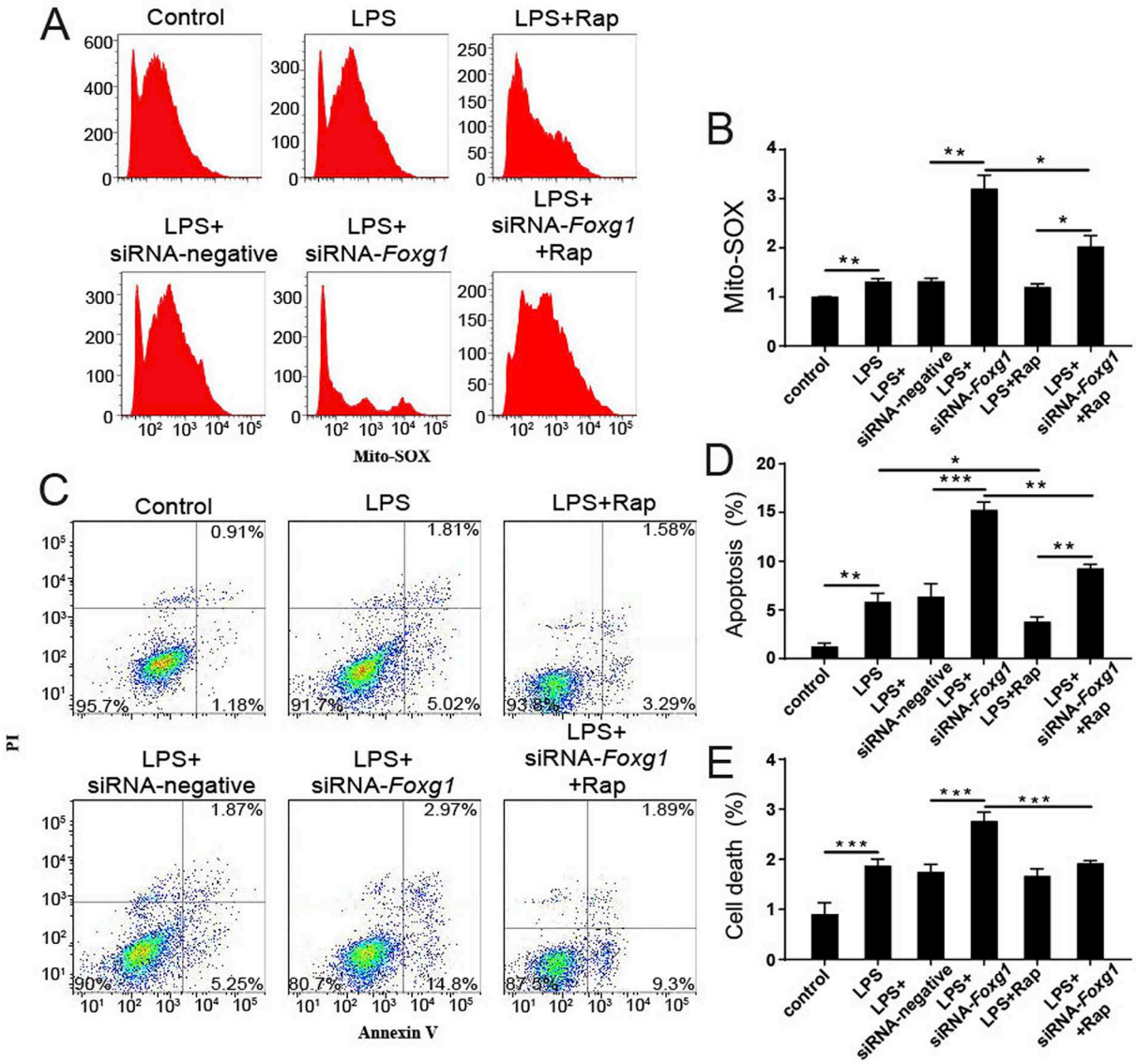


**Fig. 6.** The expression of FoxG1 affects oxidative stress and apoptosis in OC-1 cells after LPS treatment. (A) Analysis of ROS levels by flow cytometry after different treatments. (B) Quantification of the data in A. (C) Apoptosis analysis by flow cytometry after different treatments. (D) The proportions of early apoptotic cells in C. (E) The proportions of dead cells in C. *p < 0.05, **p < 0.01, ***p < 0.001.

decreasing trend in the cytoplasm of D-gal-induced aging OC-1 cells, but this was not significant (Supplement Fig. 5C–D, n = 3). These results indicated that FoxG1 might affect the process of cell aging by regulating the transcription of aging or apoptosis-related factors. Western blot also showed that the expression of FoxG1 was significantly increased in the LPS-only group and decreased in the D-gal–only group compared with controls, and the expression of FoxG1 was decreased even further in OC-1 cells co-treated with D-gal and LPS (Fig. 8A and B, $p < 0.01$, n = 3). In addition, the expression of LC3 was significantly decreased in the D-gal + LPS group compared to the LPS-only group, suggesting that the aging OC-1 cells lost their self-protection against LPS-induced inflammation (Fig. 8A and C, $p < 0.05$, n = 3).

We next measured autophagic flux using the mRFP-GFP reporter system and TEM imaging after D-gal and LPS treatment. We found that after D-gal and LPS co-treatment, the numbers of both autophagosomes and autolysosomes were decreased compared to the LPS-only group, indicating that autophagy was not activated by 1 μg/mL LPS in aging OC-1 cells (Fig. 8D–F, $p < 0.001$, n = 3). TEM imaging results were consistent with the immunofluorescence results, indicating that after D-gal and LPS co-treatment autophagic vacuoles and autolysosomes were significantly decreased compared with the LPS-only group (Fig. 8G–I, $p < 0.01$, n = 3).

### 2.12. FoxG1 regulated aging OC-1 cell survival after LPS treatment by activating the autophagy pathway

In this experiment, we downregulated FoxG1 expression in OC-1 cells to determine the role of FoxG1 in regulating the susceptibility of aging cells to LPS-induced inflammation. The flow cytometry results showed that after downregulation of *Foxg1* the proportions of both dead and apoptotic cells were significantly increased compared to the D-gal–only group (Fig. 9A–C, $p < 0.05$, n = 3). When the expression of *Foxg1* was reduced in D-gal–induced mimetic aging cells, the susceptibility to LPS-induced inflammatory injury was enhanced, resulting in significant increases in both dead and apoptotic cells compared to the D-gal + LPS group. In contrast, the proportions of both dead and apoptotic cells were significantly reduced in aging OC-1 cells when autophagy was activated by Rap after LPS-induced inflammatory injury (Fig. 9A–C, $p < 0.01$, n = 3), while the tendency of Rap to reduce apoptosis and death was decreased by inhibition of *Foxg1* expression

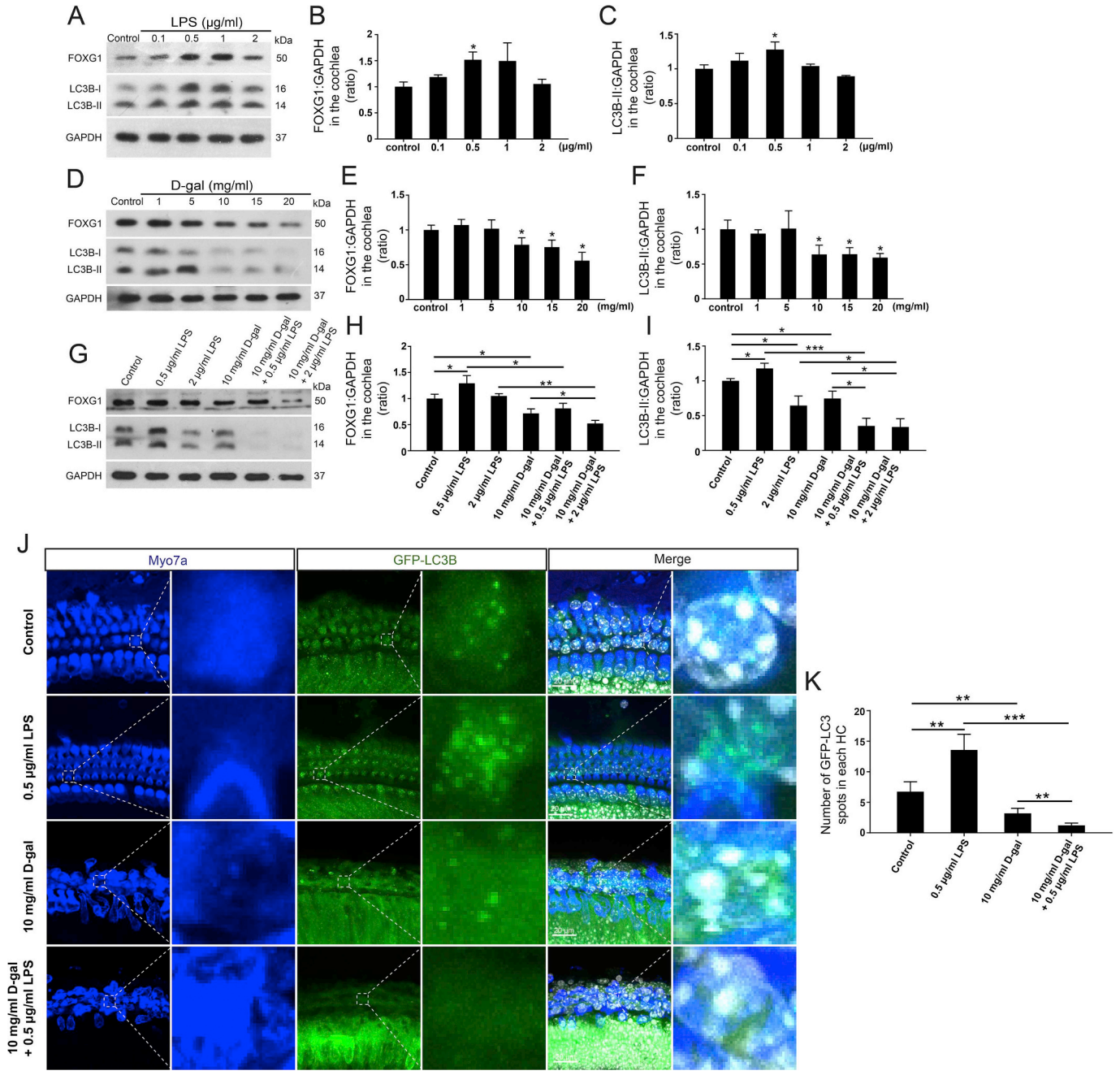


**Fig. 7.** The expression of FoxG1 affects the susceptibility to LPS-induced inflammatory response in D-gal–induced mimetic aging HCs by regulating autophagosome formation. (A) Western blot showing the changes in FoxG1 and LC3B expression in the HCs after different concentration of LPS treatment (0.1 μg/mL, 0.5 μg/mL, 1 μg/mL, and 2 μg/mL) for 48 h. (B) and (C) Quantification of the western blot in A. (D) Western blot showing the changes in FoxG1 and LC3 expression in the HCs after different concentrations of D-gal treatment (1 mg/mL, 5 mg/mL, 10 mg/mL, 15 mg/mL, and 20 mg/mL) for 72 h. (E) and (F) Quantification of the western blot in D. (G) Western blot showing the changes in FoxG1 and LC3 expression in the D-gal-induced aging HCs after LPS treatment. (H) and (I) Quantification of the western blot in G. (J) Immunofluorescence staining with Myo7a antibody in the cochleae from GFP-LC3 mice. (K) Quantification of the GFP-LC3 spot number in J. For all experiments, *p < 0.05, **p < 0.01, ***p < 0.001.

(Fig. 9A–C, $p < 0.05$, n = 3).

We also investigated whether FoxG1 affected the susceptibility to LPS-induced inflammation in D-gal–induced mimetic aging OC-1 cells by activating autophagy pathways to reduce ROS production. With the siRNA-*Foxg1* pretreatment, the ROS levels were significantly increased in aging OC-1 cells compared to the D-gal–only group and were significantly increased after LPS treatment compared to the D-gal + LPS group (Fig. 9D and E, $p < 0.01$, n = 3). In contrast, the ROS levels were significantly reduced in aging OC-1 cells after LPS treatment when autophagy was activated by Rap, while the tendency of Rap to reduce ROS accumulation was weakened by the inhibition of FoxG1 expression (Fig. 9D and E, $p < 0.05$, n = 3).

## 3. Discussion

The term “inflamm-aging” refers to low-grade, chronic inflammation that is a common clinical condition in the elderly and that might cause increased morbidity and mortality, and it is associated with many age-related diseases such as Alzheimer's disease, atherosclerosis, heart disease, type II diabetes, and cancer [50–52]. However, the precise

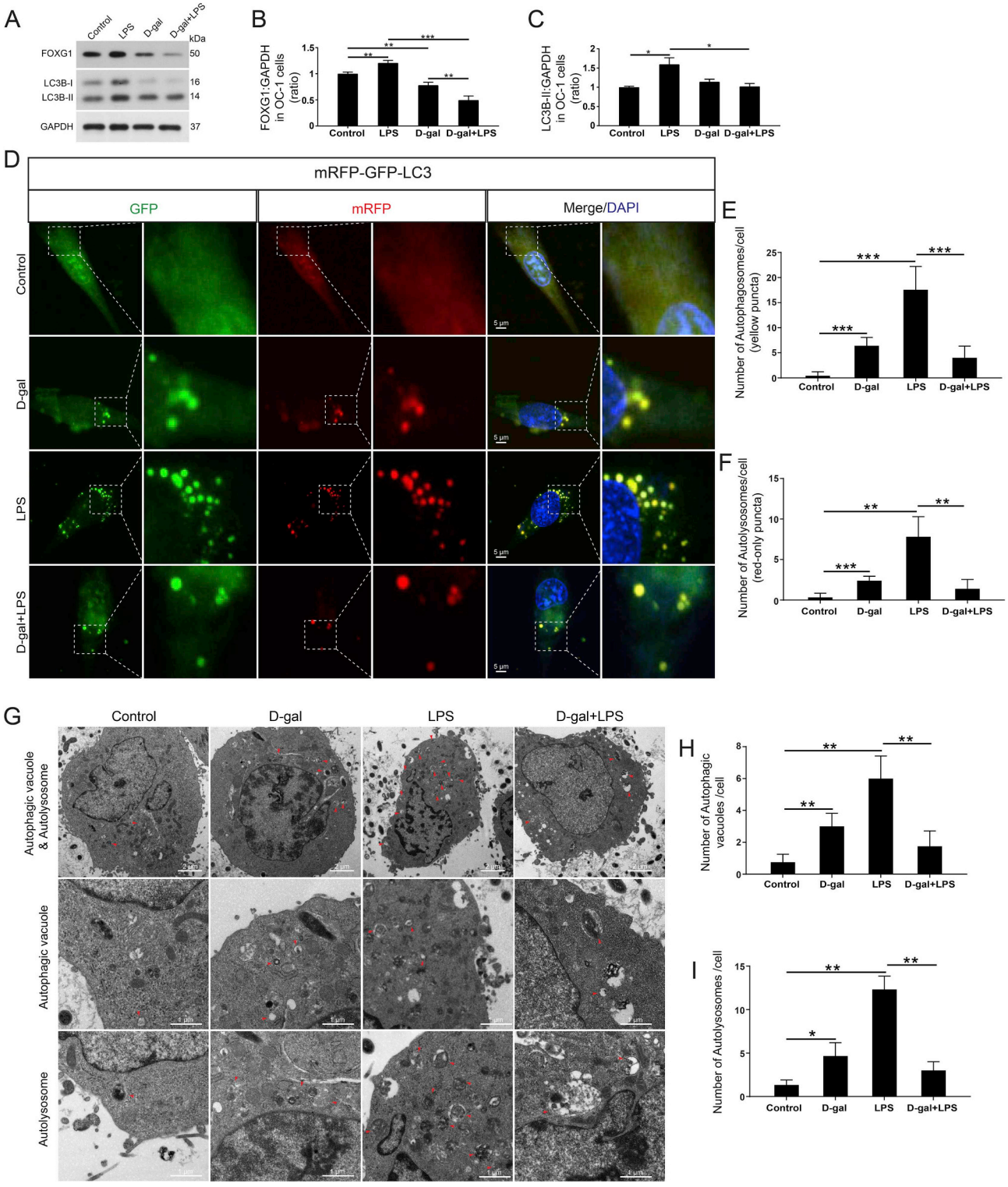


**Fig. 8.** Changes in autophagy and FoxG1 expression in D-gal–induced mimetic aging cells after LPS treatment. (A) Western blot showing the changes in FoxG1 and LC3B expression in OC-1 cells after different treatments. (B) and (C) Quantification of the western blot in A. (D) Cells were transfected with mRFP-GFP-LC3 plasmids and treated with D-gal and LPS. Yellow dots indicate autophagosomes and red dots indicate autolysosomes, n = 3. (E) Quantification of autophagosomes in D. (F) Quantification of autolysosomes in D. (G) TEM analysis for evaluating autophagy in OC-1 cells. (H) Quantification of the autophagic vacuoles in G. (I) Quantification of the autolysosomes in G. For all experiments, *p < 0.05, **p < 0.01, ***p < 0.001. (For interpretation of the references to colour in this figure legend, the reader is referred to the Web version of this article.)

etiology of inflamm-aging and its molecular mechanisms remain largely unknown.

LPS can enter the inner ear through the damaged round window membrane, and in response to this inflammatory stimulation, cells in both the middle and inner ear release cytokines that can damage the HCs [53] and lead to sensorineural hearing loss [54,55]. Therefore, it is important to determine the mechanism behind inflammation-induced HC damage. LPS induces mitochondrial damage, causes the

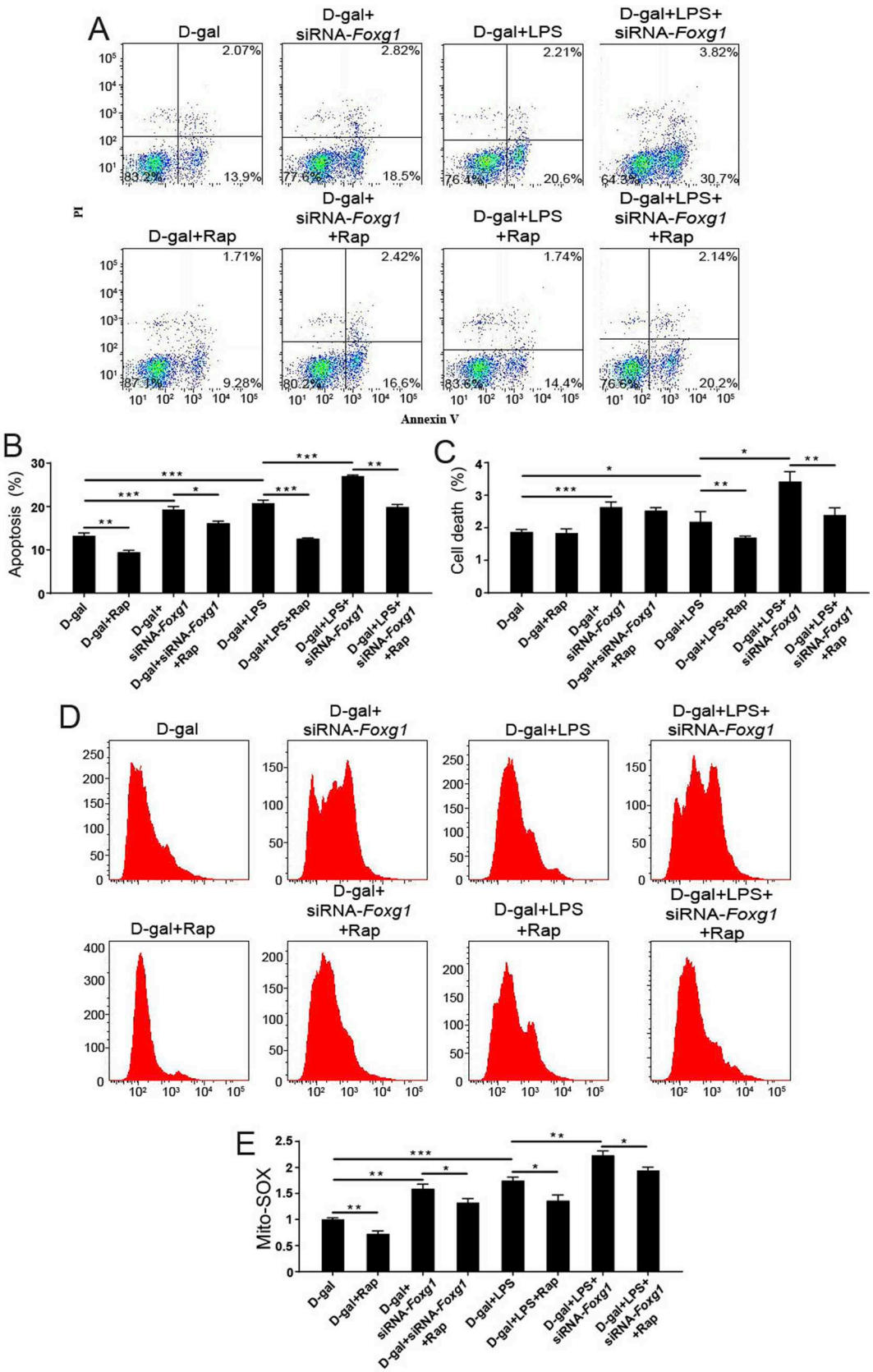


**Fig. 9.** The expression of FoxG1 affects oxidative stress and apoptosis in D-gal–induced mimetic aging OC-1 cells after D-gal and LPS treatment. (A) Apoptosis analysis by flow cytometry in *Foxg1* knockdown cells after LPS and D-gal treatment, n = 3. (B) The proportions of early apoptotic cells in A. (C) The proportions of dead cells in A. (D) Analysis of ROS levels by flow cytometry after different treatments. (E) Quantification of the data in A. *p < 0.05, **p < 0.01, ***p < 0.001.

accumulation of ROS, and activates NFKB, SAPK/JNK, caspases, and other apoptotic pathways, resulting in cell damage [56–60]. Nuclear transcription factors play a key role in the functional regulation of mitochondria, so changes in the expression levels of these proteins are closely related to the stability of mitochondrial metabolism and function [33,61,62].

As an important member of the forkhead family of transcription factors, FoxG1 plays an important role in the development, differentiation, and survival of various tissues and cells [63,64]. Our previous study also found that FoxG1 plays an important role in the regulation of HC development and survival [30], but its role in inflammation has not been reported. Here we speculated that FoxG1 might also be involved in anti-inflammatory and pro-survival processes during LPS-induced inflammation. In our in-vitro studies, we found that when HC-like OC-1 cells were treated for short times with low concentrations of LPS to induce the inflammatory response, cell viability did not change significantly, but the expression of *Foxg1* was activated. When the concentration or the treatment time of LPS increased, the expression of *Foxg1* was significantly decreased and the level of apoptosis in OC-1 cells was significantly increased. These findings need to be further investigated and verified in *in vivo* mouse models.

ROS play an important role in the inflammatory response, and mitochondria are the main site of cellular ROS production. In the excessive inflammatory response, damage to the mitochondria leads to increased mitochondrial ROS production, decreased electron transport chain activity, decreased membrane potential, ATP depletion, and decreased mtDNA copy number [65,66]. In this study, we measured the intracellular ROS content after 1 μg/mL LPS treatment for different times and found that the intracellular ROS level and the level of apoptosis both increased significantly at 72 h after treatment with LPS. When the LPS treatment time was less than 48 h, the levels of ROS and apoptosis in OC-1 cells did not increase significantly, but the expression of FoxG1 did increase significantly over the same period. We speculated that FoxG1 is likely to exert its anti-apoptotic effect by inhibiting ROS levels. Under normal conditions, ROS are produced at a low level and play an important role in signal transduction, immune response, and gene expression regulation, but excessive accumulation of ROS can be toxic to cells [66]. Upon stimulation by exogenous substances or in some diseases, the increase in ROS can activate autophagy [34,67–70].

As a survival mechanism in cells under stressful conditions, autophagy can protect cells by reducing the toxic damage of ROS to cells by eliminating organelles or proteins damaged by ROS. In this study, we found that as the duration of LPS treatment increased, the level of autophagy increased initially and then decreased, which was consistent with the changes seen in *Foxg1* expression. We thus speculate that when LPS is used to treat cells for less than 48 h, the cell's self-defense mechanism is activated, the expression of *Foxg1* is increased, and the autophagy pathway is activated to eliminate the ROS in OC-1 cells, thereby reducing the level of apoptosis. After LPS treatment for more than 48 h, the cell's self-defense capability is gradually lost, FoxG1 expression and autophagy levels are significantly decreased, and ROS and apoptosis levels increase significantly. Notably, when the expression of FoxG1 was inhibited, LPS could not activate the intracellular autophagy pathway, indicating that FoxG1 is required to activate the autophagy pathways.

Mitochondrial function is closely related to aging and inflammation [71], and mtDNA is susceptible to ROS-induced damage due to its proximity to the oxidative respiratory chain and its lack of histone protection. With the aging process, the accumulation of mitochondrial DNA damage can lead to dysfunction of the oxidative respiratory chain and to the accumulation of ROS, eventually leading to tissue damage [72,73]. As the body ages, the immune system also ages such that older individuals are more susceptible to infection and they experience greater levels of inflammation-induced tissue damage. Therefore, it is important to identify ways to resist inflammatory damage during aging.

The D-gal mimetic aging model is a common animal model of aging, and the model is designed based on the induction of metabolic disorders in the animal [74]. The animals are continuously injected with a high concentration of D-gal for a certain period of time to form galactitol under the action of aldose reductase, and this galactitol accumulates in the cells because it cannot be further metabolized, thus resulting in increased osmotic pressure and ROS accumulation [75]. D-gal increases mtDNA replication, increases the accumulation of mtDNA CD mutations, and accelerates tissue senescence [76]. Deletion of the mtDNA 4977 fragment in humans is generally thought to be associated with senile deafness, and deletion of the mtDNA4834 fragment produces the corresponding mouse model of age-related hearing loss [77]. However, the mechanism by which deletion of this mtDNA fragment leads to senile deafness remains unclear.

In our study, we used D-gal treatment in OC-1 cells and postnatal mouse cochlear explant cultures in order to construct a mimetic model of HC aging. We used the probe method to determine the mtDNA4834 fragment deletion rate, and we found a significantly increased rate in OC-1 cells treated with D-gal at a concentration of 15 mg/mL for 72 h. We also found that the mtDNA4834 fragment deletion rate in the D-gal + LPS group was significantly increased compared with the LPS-only group, while the mtDNA4834 fragment deletion rate in the D-gal + LPS group was only slightly higher than that in the D-gal–only group. In addition, we found that FoxG1 expression and autophagy levels were significantly lower in the D-gal + LPS group compared to the D-gal–only and LPS-only groups, suggesting that FoxG1 is involved in the regulation of LPS-induced inflammatory responses in aging cells. After inhibition of FoxG1 expression, the levels of ROS and apoptosis in mimetically aging cells increased significantly after LPS treatment compared with the D-gal + LPS group (Supplement Figure 6). We concluded from these results that FoxG1 affects the sensitivity of aging cells to LPS-induced inflammation through the regulation of autophagy pathways.

## 4. Materials and methods

### 4.1. Animals and treatments

In this study, P3 GFP-LC3B mice (Jackson Laboratory, 027139) were used for whole organ cochlear explant culture experiments, and P40 GFP-LC3B mice were used for *in vivo* experiments. P40 GFP-LC3B mice were injected with 2 mg/mL LPS *trans*-tympanically and sacrificed at P43 to detect the changes in FoxG1 expression and autophagy levels in HCs. All experimental procedures were carried out in accordance with the policies of the Committee on Animal Research of Tongji Medical College, Huazhong University of Science and Technology, and all efforts were made to minimize the number of mice used and their suffering. In all explant culture experiments, each group in a single experiment had no fewer than three cochlear explants, and each experiment was repeated at least three times. In the *in vivo* experiments, each experiment had at least three mice. In addition, in the HC count and autophagy detection experiments, we randomly photographed two regions of the apical, middle, and basal turns of each mouse cochlea by confocal microscopy and then collected the imaging results of multiple mice with multiple experiments and performed the statistical analysis.

### 4.2. Cell culture

In our cell culture experiments, consistent with many previous inner ear studies [78–82], we also used the HC-like OC-1 cell line, which is an immortalized cochlear sensory epithelial cell line that was derived from the organ of Corti of rats and that expresses multiple HC markers. OC-1 cells were cultured in a 37 °C incubator with 5% $CO_2$ in MEM supplemented with 20 mM HEPES, 2 mM L-glutamine, 10 mL/L non-essential amino acids, 0.4 μg/mL hydrocortisone, 5 μg/mL insulin, 2.5 μg/mL transferrin, 10 ng/mL EGF, 10% fetal bovine serum (FBS, Gibco, 10099141), 50 μg/mL streptomycin, and 50 units/mL penicillin.

Subcultures of cells were performed at 80%–90% confluence using 0.25% trypsin/EDTA (Gibco, 25200056). We designed the siRNA-*Foxg1* to knock down the expression of *Foxg1* in OC-1 cells, and an siRNA encoding a nonsense sequence was designed as the negative control. When OC-1 cells were cultivated to 50%–60% confluence in culture medium, we started to wash the cells with phosphate-buffered saline (PBS, HyClone, SH30256.01). The culture medium was replaced with Opti-MEM (Gibco, 31985062) for transfection, and OC-1 cells were transfected with siRNA following the manufacturer's instructions. About 6–8 h later, the Opti-MEM was replaced with standard MEM culture medium as described above. OC-1 cells were cultured with FBS-free culture medium with LPS or D-gal after transfection and then collected for western blot, immunofluorescence, and flow cytometry assays.

### 4.3. Cochlea explant culture

The cochlear explants were dissected and cultured as previously reported [83,84]. P3 GFP-LC3B mice were sacrificed by cervical dislocation and soaked in 75% alcohol, and the inner ear tissues including the cochlea were dissected using scissors and placed in pre-cooled sterile HBSS. The volute was opened under a microscope, and the spiral ganglion and vasculature were removed. The cochlea was then attached to the coverslip, which was pretreated with RatCol (Advanced BioMatrix, 5153), and then placed in a four-well dish. Finally, culture media was added and the explants were cultured in an incubator overnight. LPS (Sigma-Aldrich, L2880) was added for 48 h to damage the HCs. D-gal (Sigma-Aldrich, G0750, 10 mg/mL) was used to induce mimetic aging in the cochlear explants.

### 4.4. Plasmid constructs

The recombinant lentivirus vector mRFP-GFP-LC3B was produced by Hanbio Biotechnology (HB-AP2100001). In this system, a punctum with both GFP and mRFP fluorescence indicates an autophagosome that has not fused with a lysosome. Because the GFP signal is sensitive to the acidic environment when the autophagosome fuses with a lysosome, an mRFP punctum without GFP corresponds to a formative autolysosome.

### 4.5. Real-time PCR

Total RNA was extracted from OC-1 cells and whole cochleae with ExTrizol Reagent (Protein Biotechnology, PR90) and reverse transcribed to cDNA by using cDNA Synthesis Kits (Thermo Fisher Scientific, K1622) according to the manufacturers' protocols. The qRT-PCR was performed on a LightCycler 480 RT-PCR system (Roche Diagnostics Ltd, Switzerland) with the LightCycler 480 SYBR Green I Master Mix (Roche Diagnostics, 04887352001). The following primers were designed for each targeted mRNA or DNA: *FADD*, sense 5′-GCG TGA GTA AAC GAA AGC TGG-3′and antisense 5′-CAA TGT CAA ATG CCA CCC GC-3′; *Bax*, sense 5′-GTT TCA TCC AGG ATC GAG CAG A-3′ and antisense 5′-TTG TTG TCC AGT TCA TCG CCA-3′; *Aif*, sense 5′-TAG AAC TCC AGA TGG CAA GAC A-3′ and antisense 5′-AAG CCC ACA ATA AGG ACT AAC AC-3′; *Alox15*, sense 5′-TGT GGT TGG TTG GAC AGC AT-3′ and antisense 5′-TGA ATT CTG CTT CCG AGT CCC-3′; *Bcl2*, sense 5′-GAG GGG CTA CGA GTG GGA TA-3′ and antisense 5′-CGG TAG CGA CGA GAG AAG TC-3′; and *GAPDH*, sense 5′-AGT TCA ACG GCA CAG TCA A-3′ and antisense 5′-TAC TCA GCA CCA GCA TCA CC-3′. qPCR conditions consisted of an initial denaturing step of 5 min at 95 °C followed by 45 cycles of 10 s denaturation at 95 °C, 20 s annealing at 60 °C, and 20 s extension at 72 °C. The mRNA expression was normalized to the mRNA expression of GAPDH. The results were calculated using the comparative cycle threshold (ΔΔCt) method.

### 4.6. Flow cytometry

Mito-SOX Red (Thermo Fisher Scientific, M36008) was used to analyze mitochondrial ROS production. After trypsinization, OC-1 cells were collected by centrifugation and washed with cold 1 × PBS. The cell mass was then resuspended in solution containing Mito-SOX Red for 15 min at room temperature in the dark, followed by washing with cold PBS and analysis by flow cytometry within 1 h (FACSCalibur, BD Biosciences, Carlsbad, CA, USA).

FITC Annexin V (BD Biosciences, 556547) was used for the analysis of apoptosis, and propidium iodide was used to distinguish viable cells from nonviable cells. OC-1 cells were trypsinized for 5 min and collected by centrifugation at 1000 rpm for 5 min, washed with cold 1 × PBS, resuspended in 1 × binding buffer, and aliquoted at $1 \times 10^5$ cells (100 μL) into a 5 mL culture tube. FITC Annexin V and propidium iodide were added to the tube, gently vortexed, incubated for 15 min at room temperature in the dark, and analyzed by flow cytometry within 1 h.

### 4.7. Cell number analysis

OC-1 cells were cultured in 96-well plates at 2000 cells/well for 24 h, and different drugs were added with three replicates each. Cell numbers were counted with the CCK-8 Cell Counting Kit (Protein Biotechnology, CC201) at different time points. Whole organ cultured tissues were treated with different drugs, and the immunostained cells were quantified per 100 μm length of the cochlea in all three turns. The numbers of positive cells were counted in equal lengths from the middle turns of the cochleae.

### 4.8. Western blot

OC-1 cells and cochleae were lysed with cold RIPA Lysis Buffer plus PMSF. Nuclear and cytosolic protein fractions were extracted using a Nuclear/Cytosol Fractionation Kit (BioVision, K266) according to the manufacturer's protocol. A BCA Protein Quantification Kit (Beyotime Biotechnology, P0010) was used to measure the protein concentration with GAPDH as the reference protein in line with the manufacturer's instructions. LC3B-II was measured using an anti-LC3B rabbit polyclonal antibody (Sigma-Aldrich, L7543), FoxG1 was measured using an anti-FoxG1 rabbit polyclonal antibody (Abcam, ab18259), and GAPDH was measured using an anti-GAPDH rabbit polyclonal antibody (Abcam, ab8245). Peroxidase-conjugated goat anti-rabbit immunoglobulin G (Abcam, ab6721) was used as the secondary antibody. The proteins were bound to polyvinylidene fluoride membranes, and a SuperSignal West Dura chemiluminescent substrate kit was used to detect the complexes according to the manufacturer's instructions. The western blots were semi-quantified using Image J to measure the intensities of the bands.

### 4.9. Immunofluorescence

The immunohistochemistry was performed using the Fast ImmunoCytoChemistry® Staining Kit (Protein Biotechnologies). Anti-FoxG1 antibody (Abcam, ab18259), anti-LC3B antibody (Sigma-Aldrich, L7543), anti-Myosin7a antibody (Proteus Bioscience, 25–6790), a TUNEL Kit (Roche, 11684817910), and DAPI were used for analyzing FoxG1 expression and detecting autophagy, apoptotic cells, and nuclei, respectively.

### 4.10. Electron microscopy

OC-1 cells and cochleae were fixed in 2.5% glutaraldehyde (Sigma-Aldrich, G5882) for 24 h, immobilized in 1% osmic acid (Sigma-Aldrich, O5500) for 1–2 h, dehydrated with acetone (Sinopharm Chemical Reagent, u1006801), and embedded in araldite CY 212

(TAAB, E009). Ultrathin sections were stained with alcoholic uranyl acetate (Polysciences, 6159-44-0) and alkaline lead citrate (Sigma-Aldrich, 15326). The sections were washed gently with distilled water and observed with a JEM 1230 TEM (JEOL Ltd., Tokyo, Japan).

### 4.11. Statistical analysis

All data are shown as the mean ± S.D, and all experiments were repeated at least three times. Statistical analysis was conducted using Microsoft Excel and GraphPad Prism 6. Two-tailed, unpaired Student's t-tests were used to determine statistical significance when comparing two groups, and one-way ANOVA followed by a Dunnett multiple comparisons test was used when comparing more than two groups. A value of $p < 0.05$ was considered statistically significant.

## Author contributions

ZH and WK conceived and designed the experiments. ZH, SZ, ML, FL, XW, DL, and HS performed the experiments. ZH, SZ, ML, FL, XW, HS, XZ, YS, YH, RC, and WK analyzed the data. ZH, SZ, RC, and WK wrote the paper.

## Declaration of competing interest

The authors declare no competing financial interests.

## Acknowledgments

This work was supported by grants from the National Natural Science Foundation of China (Nos. 81873700, 81800915, 81230021, 81622013, 81970882, 81670929, 81400465, 81500795), the Strategic Priority Research Program of the Chinese Academy of Science (XDA16010303), the National Key R&D Program of China (Nos. 2017YFA0103903, 2015CB965000), Boehringer Ingelheim Pharma GmbH, and the Open Research Fund of the State Key Laboratory of Genetic Engineering, Fudan University, China (No. SKLGE1809).

## Appendix A. Supplementary data

Supplementary data to this article can be found online at https://doi.org/10.1016/j.redox.2019.101364.

## References

[1] G.M. Kalinec, G. Lomberk, R.A. Urrutia, F. Kalinec, Resolution of cochlear inflammation: novel target for preventing or ameliorating drug-, noise- and age-related hearing loss, Front. Cell. Neurosci. 11 (2017), https://doi.org/10.3389/fncel.2017.00192 192-192.
[2] C.R. Morales, Z. Pedrozo, S. Lavandero, J.A. Hill, Oxidative stress and autophagy in cardiovascular homeostasis, Antioxidants Redox Signal. 20 (2014) 507–518, https://doi.org/10.1089/ars.2013.5359.
[3] M.C. Calle, M.L. Fernandez, Inflammation and type 2 diabetes, Diabetes Metab. 38 (2012) 183–191, https://doi.org/10.1016/j.diabet.2011.11.006.
[4] C. Holmes, Review: systemic inflammation and Alzheimer's disease, Neuropathol. Appl. Neurobiol. 39 (2013) 51–68, https://doi.org/10.1111/j.1365-2990.2012.01307.x.
[5] N. Watson, B. Ding, X. Zhu, R.D. Frisina, Chronic inflammation - inflammaging - in the ageing cochlea: a novel target for future presbycusis therapy, Ageing Res. Rev. 40 (2017) 142–148, https://doi.org/10.1016/j.arr.2017.10.002.
[6] C.A. Verschuur, et al., Markers of inflammatory status are associated with hearing threshold in older people: findings from the Hertfordshire Ageing Study, Age Ageing 41 (2012) 92–97, https://doi.org/10.1093/ageing/afr140.
[7] Y.J. Yoon, S. Hellstrom, Ultrastructural characteristics of the round window membrane during pneumococcal otitis media in rat, J. Korean Med. Sci. 17 (2002) 230–235, https://doi.org/10.3346/jkms.2002.17.2.230.
[8] H. Kawauchi, T.F. DeMaria, D.J. Lim, Endotoxin permeability through the round window, Acta oto-laryngologica. Supplementum 457 (1989) 100–115.
[9] S.K. Juhn, et al., The role of inflammatory mediators in the pathogenesis of otitis media and sequelae, Clinical and experimental otorhinolaryngology 1 (2008) 117–138, https://doi.org/10.3342/ceo.2008.1.3.117.
[10] S. Cureoglu, P.A. Schachern, M.M. Paparella, B.R. Lindgren, Cochlear changes in chronic otitis media, The Laryngoscope 114 (2004) 622–626, https://doi.org/10.1097/00005537-200404000-00006.
[11] A.L. Smit, R.J. Stokroos, S.G. Litjens, B. Kremer, B.W. Kramer, Potential role for lipopolysaccharide in congenital sensorineural hearing loss, J. Med. Microbiol. 59 (2010) 377–383, https://doi.org/10.1099/jmm.0.015792-0.
[12] K. Hirose, C.M. Discolo, J.R. Keasler, R. Ransohoff, Mononuclear phagocytes migrate into the murine cochlea after acoustic trauma, J. Comp. Neurol. 489 (2005) 180–194.
[13] E. Sato, H.E. Shick, R.M. Ransohoff, K. Hirose, Expression of fractalkine receptor CX3CR1 on cochlear macrophages influences survival of hair cells following ototoxic injury, Journal of the Association for Research in Otolaryngology 11 (2010) 223–234.
[14] K. Hirose, S.-Z. Li, K.K. Ohlemiller, R.M. Ransohoff, Systemic lipopolysaccharide induces cochlear inflammation and exacerbates the synergistic ototoxicity of kanamycin and furosemide, Journal of the Association for Research in Otolaryngology 15 (2014) 555–570.
[15] M. Eguchi, et al., Lipopolysaccharide induces proinflammatory cytokines and chemokines in experimental otitis media through the prostaglandin D2 receptor (DP)-dependent pathway, Clin. Exp. Immunol. 163 (2011) 260–269.
[16] Y. Jiang, et al., Lipopolysaccharide disrupts the cochlear blood-labyrinth barrier by activating perivascular resident macrophages and up-regulating MMP-9, Int. J. Pediatr. Otorhinolaryngol. (2019) 109656.
[17] H. Kawauchi, T.F. Demaria, D.J. Lim, Endotoxin permeability through the round window, Acta Otolaryngol. 105 (1988) 100–115.
[18] K. WATANABE, H. HAKUHISA, Cochlear morphological changes over time after the introduction of bacterial endotoxin into the middle ear, Nippon Jibiinkoka Gakkai Kaiho 99 (1996) 1738–1745 1811.
[19] X.Z. Liu, D. Yan, Ageing and hearing loss, J. Pathol. 211 (2007) 188–197.
[20] D. Harman, Aging: a theory based on free radical and radiation chemistry, J. Gerontol. 11 (1956) 298.
[21] S. Someya, T.A. Prolla, Mitochondrial oxidative damage and apoptosis in age-related hearing loss, Mechanisms of ageing and development 131 (2010) 480–486, https://doi.org/10.1016/j.mad.2010.04.006.
[22] S. Someya, et al., The role of mtDNA mutations in the pathogenesis of age-related hearing loss in mice carrying a mutator DNA polymerase gamma, Neurobiol. Aging 29 (2008) 1080–1092, https://doi.org/10.1016/j.neurobiolaging.2007.01.014.
[23] W. Jing, et al., Mitochondrial mutations associated with aminoglycoside ototoxicity and hearing loss susceptibility identified by meta-analysis, J. Med. Genet. 52 (2015) 95–103, https://doi.org/10.1136/jmedgenet-2014-102753.
[24] J. Yu, et al., Mitochondrial DNA common deletion increases susceptibility to noise-induced hearing loss in a mimetic aging rat model, Biochem. Biophys. Res. Commun. 453 (2014) 515.
[25] S. Yu-Wen, et al., Ligustilide prevents LPS-induced iNOS expression in RAW 264.7 macrophages by preventing ROS production and down-regulating the MAPK, NF-κB and AP-1 signaling pathways, Int. Immunopharmacol. 11 (2011) 1166–1172.
[26] N. Rayamajhi, et al., Quercetin induces mitochondrial biogenesis through activation of HO-1 in HepG2 cells, Oxidative Medicine & Cellular Longevity 2013 (2013) 154279.
[27] K. Seul-Ki, et al., Resveratrol induces hepatic mitochondrial biogenesis through the sequential activation of nitric oxide and carbon monoxide production, Antioxidants Redox Signal. 20 (2014) 2589–2605.
[28] A.M. Adesina, et al., FOXG1 expression shows correlation with neuronal differentiation in cerebellar development, aggressive phenotype in medulloblastomas, and survival in a xenograft model of medulloblastoma, Hum. Pathol. 46 (2015) 1859–1871, https://doi.org/10.1016/j.humpath.2015.08.003.
[29] C.H. Hwang, A. Simeone, E. Lai, D.K. Wu, Foxg1 is required for proper separation and formation of sensory cristae during inner ear development, Dev. Dynam. : an official publication of the American Association of Anatomists 238 (2009) 2725–2734, https://doi.org/10.1002/dvdy.22111.
[30] Z. He, et al., The role of FOXG1 in the postnatal development and survival of mouse cochlear hair cells, Neuropharmacology 144 (2019) 43–57, https://doi.org/10.1016/j.neuropharm.2018.10.021.
[31] M. Brancaccio, C. Pivetta, M. Granzotto, C. Filippis, A. Mallamaci, Emx2 and Foxg1 inhibit gliogenesis and promote neuronogenesis, Stem Cells 28 (2010) 1206.
[32] S.G. Dastidar, P.M. Landrieu, S.R. D'Mello, FoxG1 promotes the survival of postmitotic neurons, Journal of Neuroscience the Official Journal of the Society for Neuroscience 31 (2011) 402.
[33] L. Pancrazi, et al., Foxg1 localizes to mitochondria and coordinates cell differentiation and bioenergetics, Proceedings of the National Academy of Sciences of the United States of America 112 (2015) 13910–13915, https://doi.org/10.1073/pnas.1515190112.
[34] Z. He, et al., Autophagy protects auditory hair cells against neomycin-induced damage, Autophagy 13 (2017) 1884–1904, https://doi.org/10.1080/15548627.2017.1359449.
[35] K. Unuma, T. Aki, T. Funakoshi, K. Hashimoto, K. Uemura, Extrusion of mitochondrial contents from lipopolysaccharide-stimulated cells: involvement of autophagy, Autophagy 11 (2015) 1520–1536, https://doi.org/10.1080/15548627.2015.1063765.
[36] R.T. Netea-Maier, T.S. Plantinga, F.L. van de Veerdonk, J.W. Smit, M.G. Netea, Modulation of inflammation by autophagy: consequences for human disease, Autophagy 12 (2016) 245–260, https://doi.org/10.1080/15548627.2015.1071759.
[37] V. Deretic, T. Saitoh, S. Akira, Autophagy in infection, inflammation and immunity, Nat. Rev. Immunol. 13 (2013) 722–737, https://doi.org/10.1038/nri3532.
[38] V. Deretic, Autophagy in infection, Curr. Opin. Cell Biol. 22 (2010) 252–262, https://doi.org/10.1016/j.ceb.2009.12.009.
[39] D.R. Green, L. Galluzzi, G. Kroemer, Mitochondria and the autophagy-

inflammation-cell death axis in organismal aging, Science (New York, N.Y.) 333 (2011) 1109–1112, https://doi.org/10.1126/science.1201940.
[40] W. Ji-Hee, P. Sangjun, H. Sujeong, S. Seunghwan, Y. Je-Wook, Rotenone-induced impairment of mitochondrial electron transport chain confers a selective priming signal for NLRP3 inflammasome activation, J. Biol. Chem. 290 (2015) 27425–27437.
[41] K. Yasui, A. Baba, Therapeutic potential of superoxide dismutase (SOD) for resolution of inflammation, Inflamm. Res. : official journal of the European Histamine Research Society ... [et al.] 55 (2006) 359.
[42] G.B. John, et al., The mitochondrial inner membrane protein mitofilin controls cristae morphology, Mol. Biol. Cell 16 (2005) 1543.
[43] K. Tracy, et al., BNIP3 is an RB/E2F target gene required for hypoxia-induced autophagy, Mol. Cell. Biol. 27 (2007) 6229–6242.
[44] K. Nakahira, et al., Autophagy proteins regulate innate immune responses by inhibiting the release of mitochondrial DNA mediated by the NALP3 inflammasome, Nat. Immunol. 12 (2011) 222.
[45] S. Kimura, T. Noda, T. Yoshimori, Dissection of the autophagosome maturation process by a novel reporter protein, tandem fluorescent-tagged LC3, Autophagy 3 (2007) 452–460, https://doi.org/10.4161/auto.4451.
[46] D.J. Klionsky, et al., Guidelines for the use and interpretation of assays for monitoring autophagy, Autophagy 8 (2012) 445–544, https://doi.org/10.4161/auto.19496.
[47] F. Zhang, J. Zhang, L. Neng, X. Shi, Characterization and inflammatory response of perivascular-resident macrophage-like melanocytes in the vestibular system, Journal of the Association for Research in Otolaryngology 14 (2013) 635–643.
[48] P. Li, D. Chen, Y. Huang, Fisetin administration improves LPS-induced acute otitis media in mouse in vivo, Int. J. Mol. Med. 42 (2018) 237–247.
[49] M.L. Golson, K.H. Kaestner, Fox transcription factors: from development to disease, Development 143 (2016) 4558–4570.
[50] S. Xia, et al., An update on inflamm-aging: mechanisms, prevention, and treatment, J. Immunol. Res. (2016) 8426874, https://doi.org/10.1155/2016/8426874 2016.
[51] A.G. Schilder, et al., Otitis media, Nature reviews. Disease primers 2 (2016) 16063, https://doi.org/10.1038/nrdp.2016.63.
[52] N.A. Francis, et al., Oral steroids for resolution of otitis media with effusion in children (OSTRICH): a double-blinded, placebo-controlled randomised trial, Lancet (London, England) 392 (2018) 557–568, https://doi.org/10.1016/s0140-6736(18)31490-9.
[53] M.J. Tarlow, S.D. Comis, M.P. Osborne, Endotoxin induced damage to the cochlea in Guinea pigs, Arch. Dis. Child. 66 (1991) 181–184, https://doi.org/10.1136/adc.66.2.181.
[54] H. Nakanishi, et al., NLRP3 mutation and cochlear autoinflammation cause syndromic and nonsyndromic hearing loss DFNA34 responsive to anakinra therapy, Proceedings of the National Academy of Sciences of the United States of America 114 (2017) E7766–e7775, https://doi.org/10.1073/pnas.1702946114.
[55] H. Tateossian, et al., Otitis media in the Tgif knockout mouse implicates TGFbeta signalling in chronic middle ear inflammatory disease, Hum. Mol. Genet. 22 (2013) 2553–2565, https://doi.org/10.1093/hmg/ddt103.
[56] J.M. Platnich, et al., Shiga toxin/lipopolysaccharide activates caspase-4 and gasdermin D to trigger mitochondrial reactive oxygen species upstream of the NLRP3 inflammasome, Cell Rep. 25 (2018) 1525–1536, https://doi.org/10.1016/j.celrep.2018.09.071 e1527.
[57] W. Abdulmahdi, et al., HMGB1 redox during sepsis, Redox biology 13 (2017) 600–607, https://doi.org/10.1016/j.redox.2017.08.001.
[58] S. da Silveira Cruz-Machado, et al., TLR4 and CD14 receptors expressed in rat pineal gland trigger NFKB pathway, J. Pineal Res. 49 (2010) 183–192, https://doi.org/10.1111/j.1600-079X.2010.00785.x.
[59] M.A. Khan, et al., JNK activation turns on LPS- and gram-negative bacteria-induced NADPH oxidase-dependent suicidal NETosis, Sci. Rep. 7 (2017) 3409, https://doi.org/10.1038/s41598-017-03257-z.
[60] M.K. Stewart, B.T. Cookson, Evasion and interference: intracellular pathogens modulate caspase-dependent inflammatory responses, Nat. Rev. Microbiol. 14 (2016) 346–359, https://doi.org/10.1038/nrmicro.2016.50.
[61] I.S. Song, et al., FOXM1-Induced PRX3 regulates stemness and survival of colon cancer cells via maintenance of mitochondrial function, Gastroenterology 149 (2015) 1006–1016, https://doi.org/10.1053/j.gastro.2015.06.007 e1009.
[62] P. Rimmele, et al., Mitochondrial metabolism in hematopoietic stem cells requires functional FOXO3, EMBO Rep. 16 (2015) 1164–1176, https://doi.org/10.15252/embr.201439704.
[63] H. Bulstrode, et al., Elevated FOXG1 and SOX2 in glioblastoma enforces neural stem cell identity through transcriptional control of cell cycle and epigenetic regulators, Genes Dev. 31 (2017) 757–773, https://doi.org/10.1101/gad.293027.116.
[64] S.T. Baek, et al., An AKT3-FOXG1-reelin network underlies defective migration in human focal malformations of cortical development, Nat. Med. 21 (2015) 1445–1454, https://doi.org/10.1038/nm.3982.
[65] L. Mela, Direct and indirect effects of endotoxin on mitochondrial function, Prog. Clin. Biol. Res. 62 (1981) 15.
[66] D.B. Zorov, M. Juhaszova, S.J. Sollott, Mitochondrial reactive oxygen species (ROS) and ROS-induced ROS release, Physiol. Rev. 94 (2014) 909–950, https://doi.org/10.1152/physrev.00026.2013.
[67] M.H. Lin, et al., Autophagy induction by the 30-100kDa fraction of areca nut in both normal and malignant cells through reactive oxygen species, Oral Oncol. 46 (2011) 822–828.
[68] Y. Chen, S.B. Gibson, Is mitochondrial generation of reactive oxygen species a trigger for autophagy? Autophagy 4 (2008) 246–248.
[69] L. Wang, et al., Distinct patterns of autophagy evoked by two benzoxazine derivatives in vascular endothelial cells, Autophagy 6 (2010) 1115–1124.
[70] M.M. Lipinski, et al., Genome-wide analysis reveals mechanisms modulating autophagy in normal brain aging and in Alzheimer's disease, Proceedings of the National Academy of Sciences of the United States of America 107 (2010) 14164–14169, https://doi.org/10.1073/pnas.1009485107.
[71] N. Sun, R.J. Youle, T. Finkel, The mitochondrial basis of aging, Mol. Cell 61 (2016) 654–666, https://doi.org/10.1016/j.molcel.2016.01.028.
[72] M. Corral-Debrinski, et al., Mitochondrial DNA deletions in human brain: regional variability and increase with advanced age, Nat. Genet. 2 (1992) 324–329, https://doi.org/10.1038/ng1292-324.
[73] M.T. Lin, D.K. Simon, C.H. Ahn, L.M. Kim, M.F. Beal, High aggregate burden of somatic mtDNA point mutations in aging and Alzheimer's disease brain, Hum. Mol. Genet. 11 (2002) 133–145.
[74] X. Song, M. Bao, D. Li, Y.M. Li, Advanced glycation in D-galactose induced mouse aging model, Mechanisms of ageing and development 108 (1999) 239–251.
[75] Z. Du, et al., A long-term high-fat diet increases oxidative stress, mitochondrial damage and apoptosis in the inner ear of D-galactose-induced aging rats, Hear. Res. 287 (2012) 15–24, https://doi.org/10.1016/j.heares.2012.04.012.
[76] Y. Zhong, et al., Contribution of common deletion to total deletion burden in mitochondrial DNA from inner ear of d-galactose-induced aging rats, Mutat. Res. 712 (2011) 11–19, https://doi.org/10.1016/j.mrfmmm.2011.03.013.
[77] W.J. Kong, et al., The effect of the mtDNA4834 deletion on hearing, Biochem. Biophys. Res. Commun. 344 (2006) 425–430, https://doi.org/10.1016/j.bbrc.2006.03.060.
[78] M.N. Rivolta, M.C. Holley, Cell lines in inner ear research, J. Neurobiol. 53 (2002) 306–318.
[79] Y. Zheng, et al., EGF mediates survival of rat cochlear sensory cells via an NF-κB dependent mechanism in vitro, Open Neurosci. J. 2 (2008) 9.
[80] J. Chen, et al., Id1/NR2B receptor pathway regulates rat cochlear sensory epithelial cell survival after radiation, Audiology and Neurotology 23 (2018) 173–180.
[81] M. Ozeki, et al., Establishment and characterization of rat progenitor hair cell lines, Hear. Res. 179 (2003) 43–52.
[82] M. Ozeki, et al., Id1 induces the proliferation of cochlear sensory epithelial cells via the nuclear factor-κB/cyclin D1 pathway in vitro, J. Neurosci. Res. 85 (2007) 515–524.
[83] C.-H. Yang, et al., Histone deacetylase inhibitors are protective in acute but not in chronic models of ototoxicity, Front. Cell. Neurosci. 11 (2017) 315.
[84] Y. Chen, et al., Cotransfection of Pax2 and Math1 promote in situ cochlear hair cell regeneration after neomycin insult, Sci. Rep. 3 (2013) 2996.